WHITE PAPER

Pharmacology Discovery Services
A Eurofins Discovery Partner Lab

eurofins | DISCOVERY

NASH DRUG DISCOVERY

Select the Appropriate *In Vitro* Assays and *In Vivo* Models for Your NASH Drug Discovery Program

Authors: Eurofins Discovery: Phil Lin, MS; Pharmacology Discovery Services: Tai-Yu Huang, MS, Jimmy Bao, PhD.

GLOBAL INCIDENCE OF NON-ALCOHOLIC STEATOHEPATITIS (NASH)

Non-alcoholic fatty liver (NAFL) is a condition that is expected to become more common as the rates of obesity and Type II diabetes increase globally. NAFL has many potential pathologies, and it can progress to a more serious condition, non-alcoholic steatohepatitis (NASH) that may result in liver fibrosis, cirrhosis, or hepatocellular carcinoma. NASH has become a leading cause of cirrhosis with a death rate that has held constant since 1990, while other leading causes of cirrhosis (hepatitis B/C and alcohol-related liver disease) have seen decreases in death rates over the same period.[1] As the global incidence of NALF is projected to increase, cases of NASH are expected to increase from 16.5 million cases in 2015 to 27 million cases by 2030.[2] With increasing rates of NASH, and the difficulty in prevention or early diagnosis of the disease, the need for therapeutic intervention to impede the progression of NAFL to severe cases of NASH will become more necessary.

> NASH is a leading cause of cirrhosis with a death rate that has held constant since 1990. Other causes of cirrhosis (hepatitis and alcohol-related disease) have seen decreases in death rates over that same period.

PATHOGENESIS OF NAFL TO NASH

The progression of NAFL to NASH, which can lead to liver fibrosis and cirrhosis, is highly complex, and the primary drivers of disease progression remain unclear. NAFL can lead to NASH with the development of hepatic inflammation and hepatocyte damage (e.g., steatohepatitis). Quite often, NASH is accompanied by pericellular fibrosis, which in the most serious clinical cases may lead to cirrhosis. Current thought on the pathogenesis of NALF to NASH includes a variety of factors: diet, obesity, microbiome, and genetic predisposition with respect to the accumulation of triglycerides and other lipids in hepatocytes. A two-hit model or multiple-hit model has been proposed to explain the development of NAFL disease.[4,5] The first hit is the initial hepatic lipid accumulation, but a second hit is required for progression to liver injury, inflammation, and fibrosis (Figure 1). Hepatic oxidative stress is likely the main factor for the second hit that could cause cellular injury and trigger the recruitment of inflammatory cells.

Until the complex pathogenesis of NASH is better understood, the range of potential therapeutic targets will be diverse. Existing drug candidates in development for NASH include farnesoid X receptor (FXR) agonists, PPARα/δ agonists, ASK-1 inhibitors, glucagon-like peptide 1 analogues, fibroblast growth factor 19 and 21 analogues, galectin-3 antagonists, acetyl-coenzyme A carboxylase (ACC) inhibitors, and thyroid hormone receptor-β selective thyromimetics.[3,7] These targets have relevance for what are the four most likely disease mechanisms of NASH: hepatic steatosis, insulin resistance, chronic inflammation, and fibrosis. The complexity of NASH pathogenesis also indicates that combination therapies, as opposed to monotherapies, could become a successful therapeutic strategy.

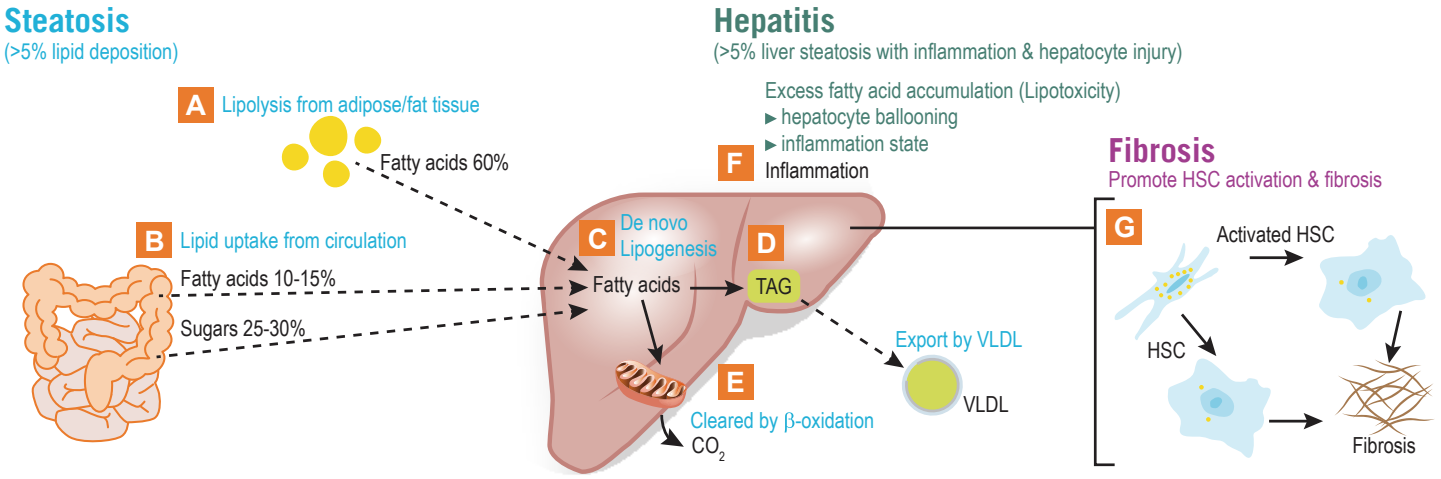

Figure 1. Lipid metabolism and NASH progression. A. The free fatty acids are released via lipolysis from adipocyte and fat tissue, B. lipid uptake from circulation, (C. and D.) *de novo* lipogenesis from sugars to triacylglycerol. These three pathways are the primary source of hepatic lipids. E. Lipids are cleared by β-oxidation via mitochondria and exported by very low-density lipoprotein (VLDL). Pathogenesis of NAFL is owing to the accumulation of fatty acids (>5%), which results in lipotoxicity in the hepatocytes (steatosis). NASH is a more progressive form of liver steatosis. F. Progressive liver injury caused by lipotoxicity leads to hepatocyte ballooning and activation of inflammatory responses (hepatitis). G. The inflammatory response stimulates the activation of hepatic stellate cells (HSCs) and generates extensive extracellular matrix (ECM) remodeling, leading to more severe liver fibrosis. The figure is modified from Esler WP and Bence, KK, 2019.[6]

IN VITRO PANELS FOR NASH DRUG DISCOVERY

Eurofins Discovery has three *in vitro* panels that may be used to identify hits for NASH drug discovery. The panels are relevant for candidates that target liver steatosis, hepatitis, and liver fibrosis. To highlight the diversity of NASH pathogenesis, these panels include 26 targets in diverse target classes, with every target having at least one drug candidate in clinical development.[8,9,10] Depending on the relevant assay technology for each target, the panels have a combination of binding, enzymatic, functional, or phenotypic assays. Any of the assays in these panels can be ordered individually. All assays are well-characterized with reference compounds and reported clinical candidates (Figures 2–4).

LIVER STEATOSIS LEADHUNTER PANEL

This panel (Item #PP270) contains 13 targets across six target classes that play a role in hepatic fat accumulation. The assays in this panel can be ordered individually.

Class	Target	MOA	Biological Relevance
Carboxylase	ACC1	Inhibitor	ACC1 controls fatty acid biosynthesis and metabolism, ACC1 inhibition can limit fatty acid synthesis while simultaneously triggering fatty acid oxidation.
GPCR	GLP1R	Activator	GLP1R activation via GLP1 limits ER stress, activates AMPK, and dampens lipogenesis. Several GLP1R analogues have been approved for Type II Diabetes.
	TGR5		TGR5 activation induces systemic release of glucagon-like peptides (GLP-1 & -2), which are key modulators for glucose metabolism.
Kinase	AMPK	Activator	AMPK activation regulates lipid homeostasis, glycolysis, and mitochondrial homeostasis. AMPK activation inhibits ACC1/2 activity, which are major regulators in lipid metabolism.
	FGFR1		FGF21-FGFR1 activation stimulates fatty acid oxidation leading to hepatic fat reduction. FGF21 also increases adiponectin levels.
	FGFR4		FGF19-FGFR1/4 activation inhibits insulin-induced hepatic lipogenesis, increases fatty acid oxidation and metabolic rate leading to fat mass reduction.
Lipase	Pancreatic Lipase	Inhibitor	Targeting pancreatic lipase (e.g., Orlistat) exhibits lower fasting glucose and improved insulin resistance along with weight loss.
NHR	FXR	Activator	FXR plays crucial roles in the regulation of bile acid (BA) synthesis, secretion, and transport. FXR also regulates lipid and glucose metabolism.
	PPARα		PPARα regulates fatty acid oxidation and ketogenesis.
	PPARδ		PPARδ controls fatty acid metabolism and inflammation.
	PPARγ		PPARγ regulates adipocyte differentiation and lipogenesis
	THRβ		THR regulates energy metabolism, lipid utilization, and glucose homeostasis. THRβ is the major isoform expressed in the liver.
Transporter	IBAT	Inhibitor	95% of secreted BAs are recirculated back to the liver via IBAT, which is also known as enterohepatic circulation (EC). Interruption of EC by IBAT inhibitors reduces inflammatory/ fibrogenic gens expression and hepatic TG levels.

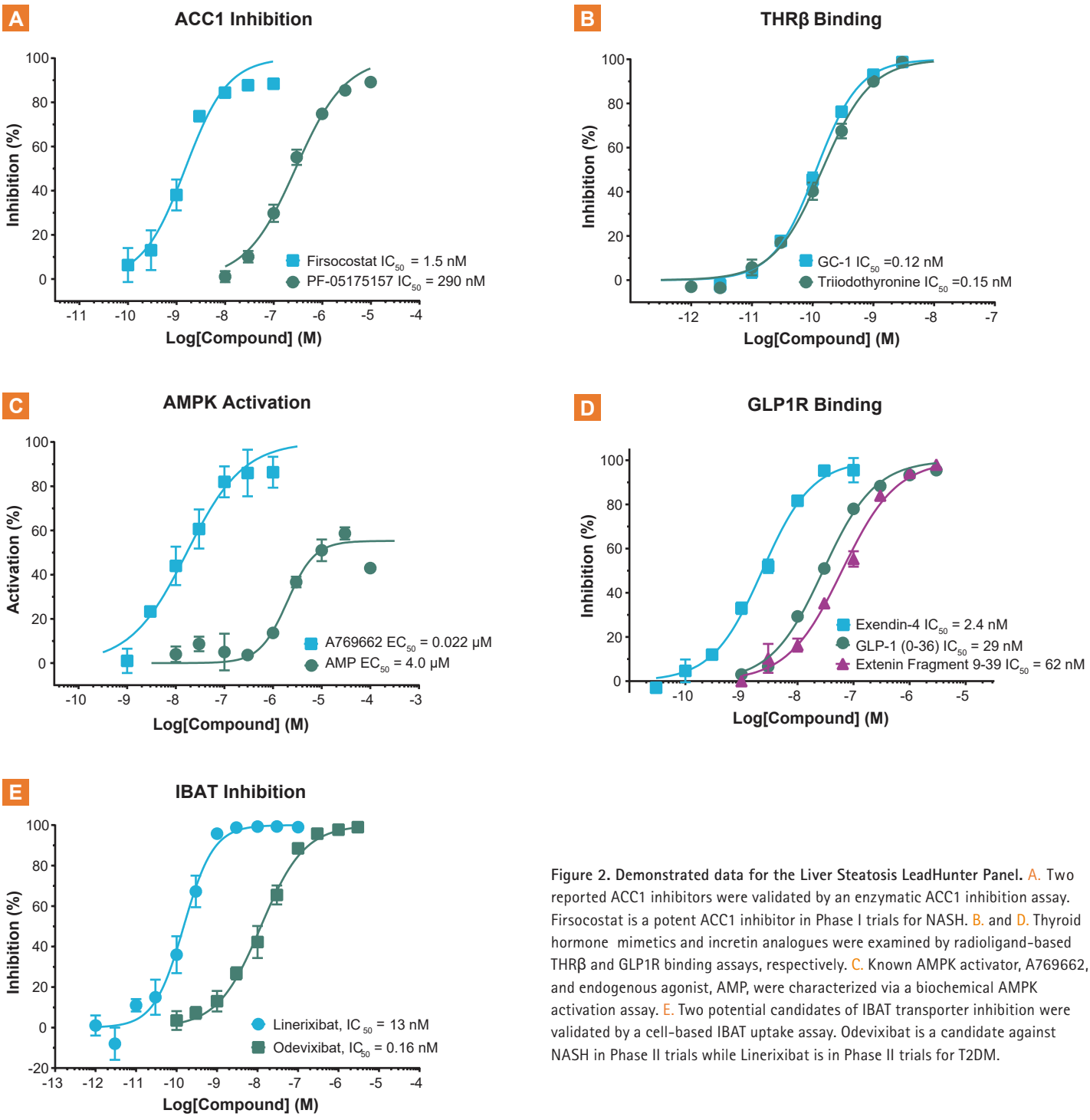

Figure 2. Demonstrated data for the Liver Steatosis LeadHunter Panel. A. Two reported ACC1 inhibitors were validated by an enzymatic ACC1 inhibition assay. Firsocostat is a potent ACC1 inhibitor in Phase I trials for NASH. B. and D. Thyroid hormone mimetics and incretin analogues were examined by radioligand-based THRβ and GLP1R binding assays, respectively. C. Known AMPK activator, A769662, and endogenous agonist, AMP, were characterized via a biochemical AMPK activation assay. E. Two potential candidates of IBAT transporter inhibition were validated by a cell-based IBAT uptake assay. Odevixibat is a candidate against NASH in Phase II trials while Linerixibat is in Phase II trials for T2DM.

HEPATITIS LEADHUNTER PANEL

This panel (Item #PP271) contains 11 targets across six target classes that play a role in the development of hepatitis. The assays in this panel can be ordered individually.

Class	Target	MOA	Biological Relevance
Caspase	Caspase 3	Inhibitor	Caspases regulate cellular inflammatory response and cell apoptosis to maintain organ homeostasis. Caspase-dependent apoptosis is involved in the progression of severe NASH.
	Caspase 7		
	Caspase 8		
GPCR	CCR2	Inhibitor	CCR2 macrophages accumulate in patients with NASH and advanced fibrosis, which promotes inflammation and directly stimulates hepatic stellate cell activation.
	CCR5		CCR5 is expressed in lymphocyte and hepatic stellate cells, where it regulates migration and proliferation.
	CysLT1		Inhibiting CysLT1 shows anti-inflammatory and anti-oxidant responses in hepatocytes.
Kinase	ASK1	Inhibitor	ASK1 is a key enzyme that promotes apoptosis, inflammation, and fibrosis through JNK and p38 pathways.
Oxidase	VAP-1	Inhibitor	VAP-1 is directly involved in hepatic stellate cell activation and is a strong pro-fibrogenic stimulator.
PDE	PDE4A	Inhibitor	PDE4 is an intracellular enzyme that modulates inflammation and epithelial integrity. PDE4 inhibition elevates cAMP levels and modulates inflammatory responses.
	PDE4B		
Transcription Factor	Nrf2	Activator	Nrf2 is a crucial regulator for cellular protection by inducing anti-inflammatory and anti-oxidant gene expression.

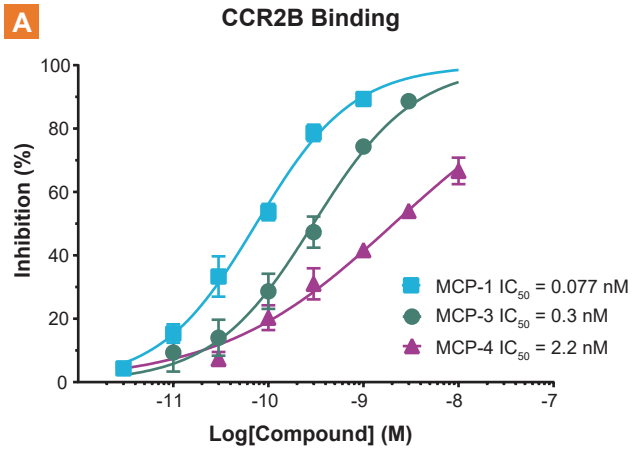

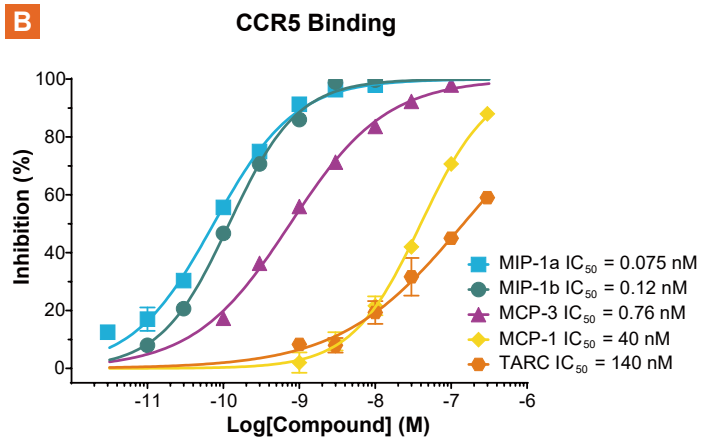

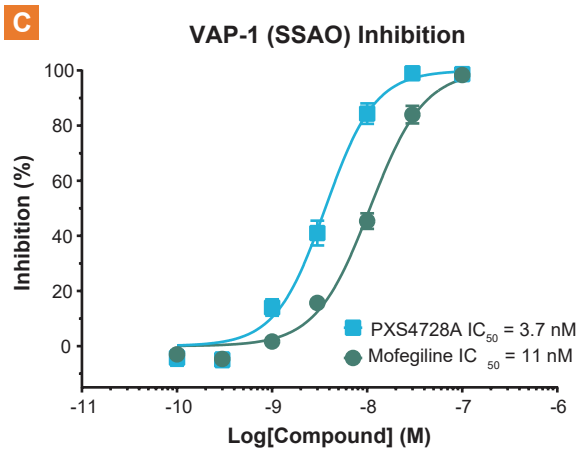

Figure 3. Demonstrated data for the Hepatitis LeadHunter Panel. A. and B. Binding of the known CCR2 and CCR5 agonists was validated by radioligand-based binding assays. C. Reported VAP-1 inhibitors were examined by an enzymatic VAP-1 inhibition assay. PXS4728A is a Phase II candidate for NASH.

LIVER FIBROSIS LEADHUNTER PANEL

This panel (Item #PP272) contains two assays to evaluate the anti-fibrotic activity of drug candidates. The assays in this panel can be ordered individually.

Class	Target	MOA	Biological Relevance
Oxidase	LOXL2	Inhibitor	LOXL2 functions as a regulator to promote the network of extracellular matrix collagen fibers, and it plays a key role in the pathogenesis of liver fibrosis.
Phenotypic	Liver Fibrosis Model	Inhibitor	Human hepatic stellate cell line, LX-2, is induced by TGFβ and the fibrogenic marker COL1A1 is detected by high-content analysis.

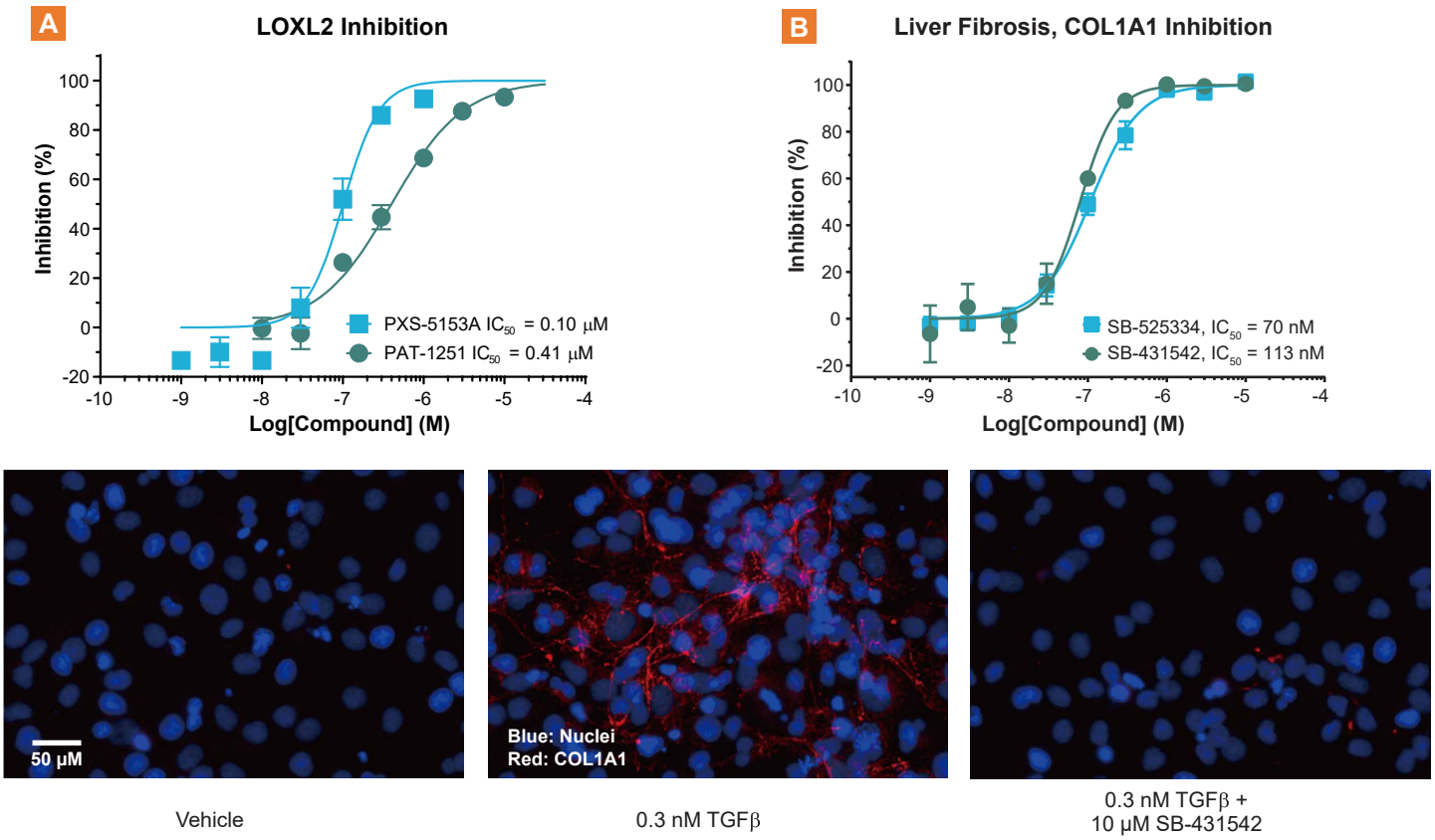

Figure 4. Demonstrated data for the Liver Fibrosis LeadHunter Panel. A. ECM remodeling enzyme, LOXL2, was measured by the IC_{50} of two inhibitors by an enzymatic LOXL2 inhibition assay. PAT-1251 is in Phase I trials for lung fibrosis. B. Human HSC LX-2 cells were activated by 0.3 nM TGFβ for 48-hr. C. Fibrogenesis was monitored by evaluating the fibrogenic marker collagen, type 1, α1 (COL1A1) expression level and analyzed by high-content imaging (Blue: Nuclei; Red: COL1A1). TGFβ successfully induced liver fibrosis with a high level of COL1A1 expression (Image, middle). Induced COL1A1 expression was dose-dependently inhibited by two TGFβ inhibitors, SB-525334 and SB-431542, respectively.

IN VIVO MODELS OF NASH FROM PHARMACOLOGY DISCOVERY SERVICES

The ideal preclinical animal model of NASH would reproducibly mimic the diverse disease pathogenesis that is observed in the clinic in a timely manner. This includes obesity, insulin resistance, hepatic fat accumulation, and the specific characteristics of NASH that include liver steatosis, hepatocyte inflammation, lobular inflammation, and liver fibrosis.[11] There are dozens of published models of NASH, diet-induced or genetically-induced models are the most common. Due to the complexity of NASH pathogenesis, and the availability of dozens of different models, there is not a consensus on which models are most appropriate. Genetically modified models such as leptin-deficient (ob/ob) or leptin-resistant (db/db) mouse and the dietary methionine- and choline-deficient (MCD) model are most commonly used in the literature.[12] This makes selecting an appropriate preclinical NASH model based on specific study objectives the optimal strategy.

Pharmacology Discovery Services (PDS) has two diet-induced rodent models of NASH. The first is the Methionine- and Choline-deficient (MCD) model, and the second is the Choline-deficient, L-amino acid-defined, High-fat Diet (CDAHFD) model, both in C57BL/6 mice, which are sensitive to high-fat diet-induced obesity or NASH. Both of these models rely upon lipotropic deficiency (methionine and/or choline) that impedes normal intrahepatic triglyceride metabolism since choline deficiency leads to impaired secretion of very low-density lipoprotein (VLDL), which contains an abundance of triglycerides. This leads to steatosis, oxidative stress, and liver cell death.[13] The MCD and CDAHFD models successfully induce hepatic steatosis, inflammation, and liver fibrosis. A key difference between these two models is that the MCD model results in weight loss while the CDAHFD model is able to maintain body weight throughout a study. Another difference in these models is the time required for the induction of fibrosis. The CDAHFD models require approximately four additional weeks for induction relative to the MCD model. Neither model is able to replicate obesity or insulin resistance, whichare common metabolic characteristics of NASH in humans.[14,15,16]

Due to the species difference between mice and human, we have recently also developed a NASH model in humanized liver chimeric mouse (HLCM), in which mouse liver is highly replaced by human hepatocytes, developed by PhoenixBio. We have validated this model using a clinically effective drug, obeticholic acid (OCA), a farnesoid X receptor (FXR) agonist, effective in treating NASH in late clinical trials. This model is more clinically translational and could be offered a more relevant animal model for testing anti-NASH therapeutics.

Due to the complexity of NASH pathogenesis, there is not consensus on what *in vivo* models are most appropriate. Selecting a model based on specific study objectives is the optimal strategy.

MCD DIET-INDUCED NASH MODEL IN C57BL/6 MICE

The mouse MCD diet-induced NASH model rapidly elicits pathogenesis in the liver (e.g., 4-8 weeks) that is similar to NASH in humans. Liver steatosis and inflammation develop, and this leads to liver fibrosis in a reliable and relatively quick time frame. The MCD model is considered the best-established model to study inflammatory and fibrotic processes. It is especially useful for the study of histologically advanced NASH and the mechanisms of inflammation and fibrosis.[12, 17] Drawbacks of the MCD model include body weight loss, liver atrophy, and a metabolic profile (e.g., lack of insulin resistance) that diverges from NASH in humans.[12] When clients determine if the MCD model is appropriate for their study, they should first determine if these profiles for the model are acceptable.

MCD MODEL IN C57BL/6 MICE PROTOCOL

Groups of 10 male C57BL/6 mice at 8-10 weeks of age are used. Mice are fed a methionine- and choline-deficient (MCD) diet or control diet for 4 or 8 weeks. Vehicle and test articles are administered orally by gavage to mice daily during the 4 or 8 weeks of diet feeding. Body weight, liver weight, biochemical analysis, and histological changes are assessed after 4 or 8 weeks of MCD diet feeding. Plasma alanine aminotransferase (ALT) and aspartate aminotransferase (AST) levels are measured at weeks 4 and/or 8.

The animals are sacrificed 24 hours after the final treatment, and the liver is harvested and weighed. Liver-to-body weight ratio is then calculated for each animal according to the formula: Liver (g)/BW x 100. Half of the liver is snapped frozen in liquid N_2 for further study, and the remaining 1/2 portion is formalin-fixed for histology.

The readouts that are available from PDS for the MCD model include: body weight, ALT, AST, ALP, T-BIL and ALB levels, liver weight, biomarker analysis (protein or mRNA), and histopathology.

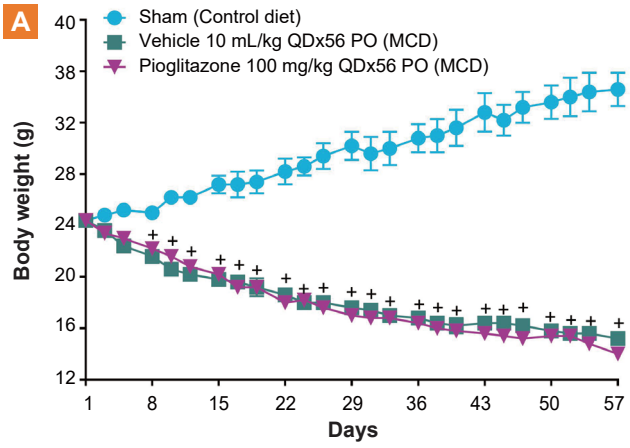

+p < 0.05, vehicle vs. sham control; Two-way ANOVA followed by Bonferroni test.

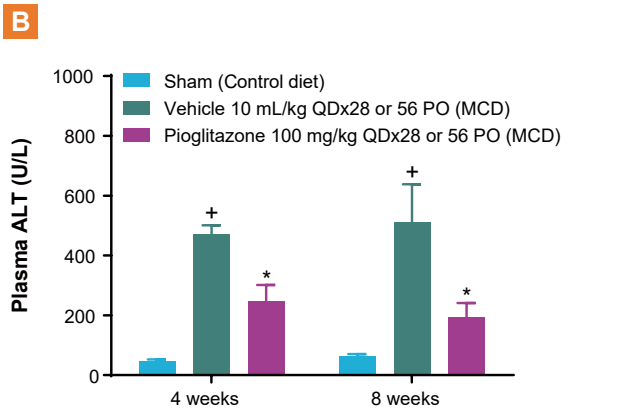

+p < 0.05, vehicle vs. sham control; *p < 0.05, treated vs. vehicle control; Two-way ANOVA followed by Bonferroni test.

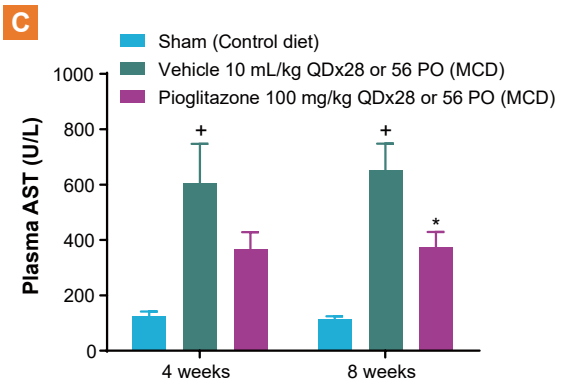

+p < 0.05, vehicle vs. sham control; *p < 0.05, treated vs. vehicle control; Two-way ANOVA followed by Bonferroni test.

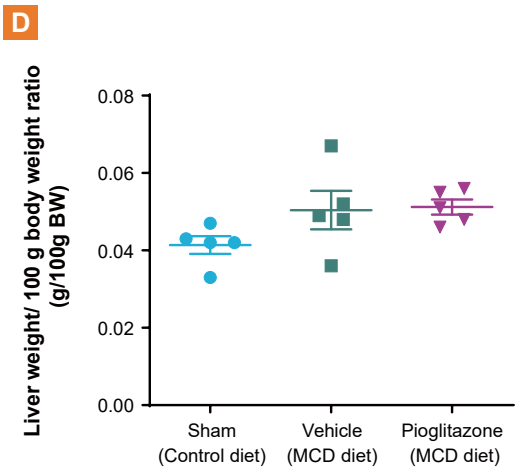

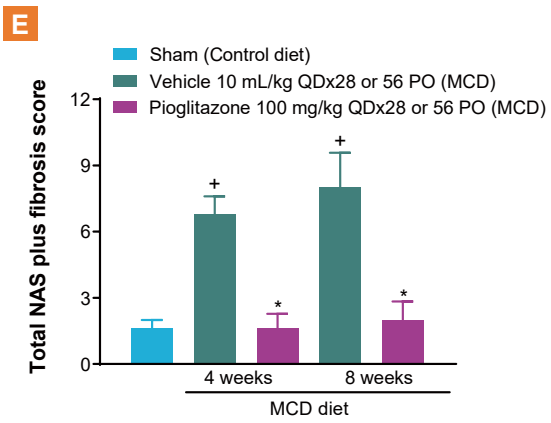

+p < 0.05, vehicle vs. sham control; *p < 0.05, treated vs. vehicle control; One-way ANOVA followed by Dunnett's test.

Figure 5. Demonstrated data for the MCD Diet-induced NASH Model. A. Body weight. B. Plasma ALT levels. C. Plasma AST levels. D. Liver Weight/ Body Weight Ratio. E. Total NAS plus fibrosis score.

CDAHFD-INDUCED NASH MODEL IN C57BL/6 MICE

High-fat diets (HFD) in mice produce NAFL and obesity but fail to elicit other pathologies of NASH, most importantly liver fibrosis and cirrhosis. The choline-deficient, L-amino acid-defined, high-fat diet (CDAHFD) model has a diet with an optimized level of methionine.[18] This differs from the MCD diet-induced model that is deficient in both methionine and choline. A key feature of the CDAHFD model is that weight loss is not observed (Figure 6) even up to 60 weeks, in contrast to the MCD diet-induced NASH model (Figure 5).[19] Mice fed CDAHFD show a histopathological progression from steatosis, NASH, and fibrosis over a 12-week study period, which nicely resembles the human NASH phenotype.[20] The primary drawback with the CDAHFD model is that it lacks the metabolic profile (e.g., hypertriglyceridemia and hyperglycemia) that is observed in human NASH.

CDAHFD MODEL IN C57BL/6 MICE PROTOCOL

Mice are fed a choline-deficient, amino acid-defined high-fat diet (CDAHFD) or control diet for 12 weeks. Vehicle and test articles are administered by oral gavage once daily during the 12 weeks of diet feeding. Serum alanine aminotransferase (ALT) and aspartate aminotransferase (AST) levels are determined for evaluation of hepatic impairment on Days 14, 28, 42, 56, 70, and 84.

At termination (Day 84), animals are sacrificed 24 hours after the final treatment, and the livers are harvested and weighed. Liver-to-body weight ratio is then calculated for each animal according to the formula: Liver (g)/BW x 100. Half of the liver is snap frozen in liquid N_2 for further cytokine analysis (optional), and the remaining 1/2 portion is formalin-fixed for histopathology (optional).

The readouts that are available from PDS for the CDAHFD model include: body weight, ALT, AST, ALP, T-BIL and ALB levels, liver weight, biomarker analysis (protein or mRNA), and histopathology.

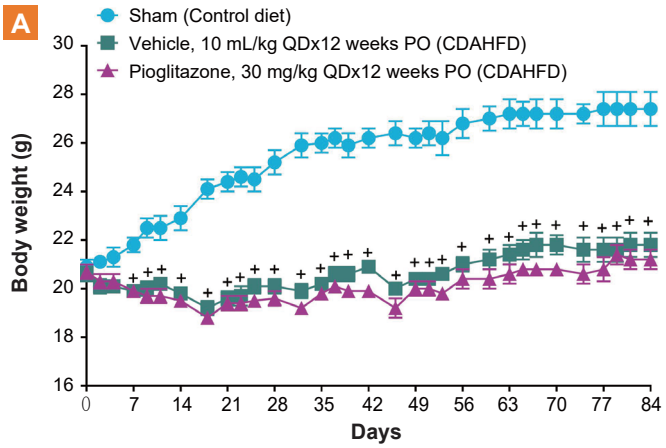

+p < 0.05, vehicle vs. sham control; Two-way ANOVA followed by Bonferroni test.

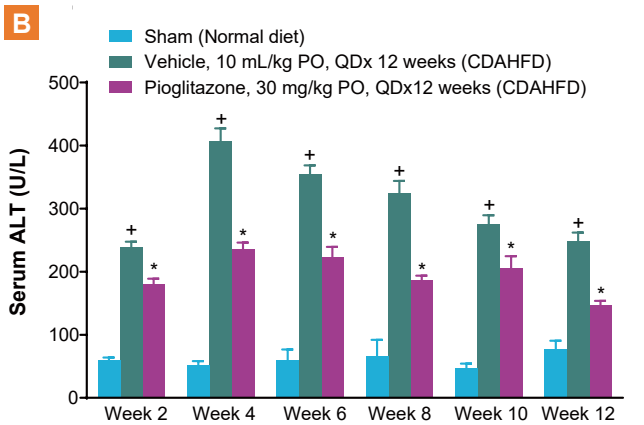

+p < 0.05, vehicle vs. sham control; * p < 0.05, treated vs. vehicle control; Two-way ANOVA followed by Bonferroni test.

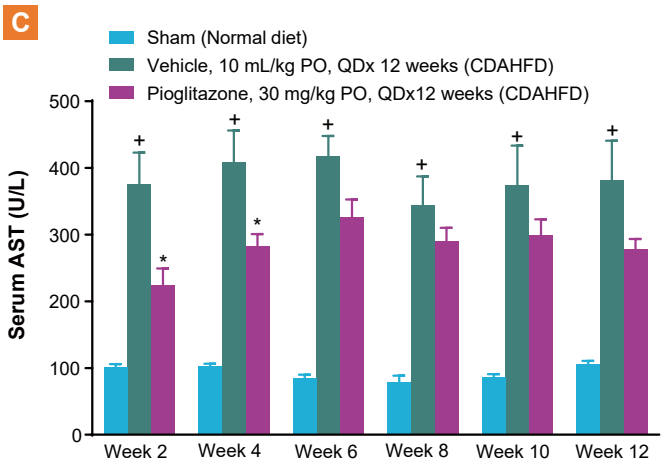

+p < 0.05, vehicle vs. sham control; * p < 0.05, treated vs. vehicle control; Two-way ANOVA followed by Bonferroni test.

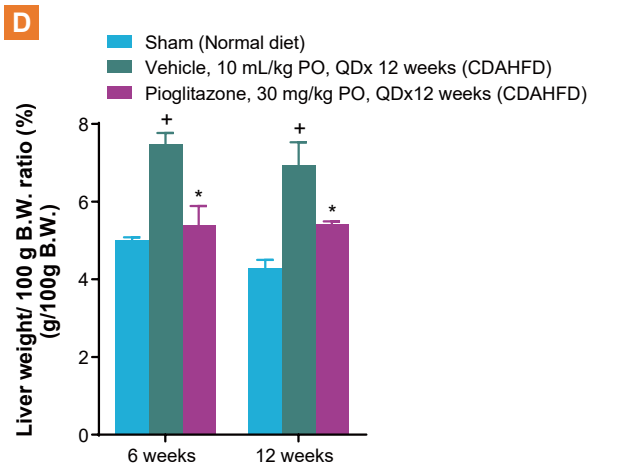

+p < 0.05, vehicle vs. sham control; * p < 0.05, treated vs. vehicle control; Two-way ANOVA followed by Bonferroni test.

CDAHFD MODEL PROTOCOL ...continued

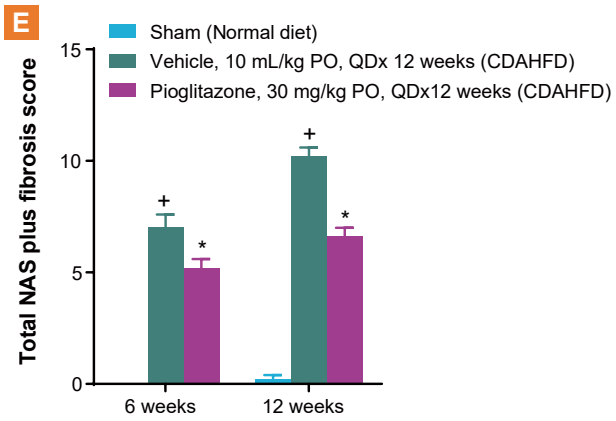

+p < 0.05, vehicle vs. sham control; *p < 0.05, treated vs. vehicle control; Two-way ANOVA followed by Bonferroni test.

Figure 6. Demonstrated data in the CDAHFD-induced NASH model. A. Body weight. B. Serum ALT levels. C. Serum AST levels. D. Liver Weight/Body Weight Ratio. E. Total NAS plus fibrosis score.

CDAHFD-INDUCED NASH MODEL IN HUMANIZED LIVER CHIMERIC MICE

Humanized liver chimeric mice (HLCM) have been created in which mouse hepatocytes are largely replaced by human hepatocytes and have been used for drug metabolism, pharmacokinetic studies, liver toxicity testing, drug transport, and drug-drug interactions.[21] There are three main HLCM platforms, namely cDNA-uPA/SCID mice, also known as PXB-mice, $Fah^{-/-}Rag2^{-/-}Il2r\gamma^{-/-}$ (or FRG mice), and HSV-TK-NOG (or TK-NOG mice), with PXB-mice having the following advantages: higher replacement index within a relatively short period of time, intact innate immune system, and better-preserved hepatic structure.[22] We have used PXB-mice to develop the NASH model and validated the model using a clinically effective drug candidate, obeticholic acid (OCA).

Consistent with the literature report, PXB-mice, after CDAHFD feeding, develop liver injury, increased hepatic lipid accumulation, liver steatosis, hepatocellular ballooning with the formation of Mallory-Denk bodies, and liver fibrosis, features of human NASH.[23] OCA treated prophylactically significantly reduced all these (Figure 7). It is thus believed that the NASH model in HLCM is more clinically relevant and would be used more and more in the late pre-clinical development of NASH drug candidates.

CDAHFD MODEL IN HUMANIZED LIVER CHIMERIC MICE PROTOCOL

Mice are fed a choline-deficient, amino acid-defined high-fat diet (CDAHFD) or control diet (CRF-1 diet) for 12 weeks. Vehicle and test articles are administered by oral gavage once daily during the 12 weeks of diet feeding. Serum alanine aminotransferase (ALT) and aspartate aminotransferase (AST) levels are determined for evaluation of hepatic impairment on Weeks 2, 4, 6, 8, 10, and 12.

Animals are sacrificed at Week 12, and the livers are harvested and weighed. Liver-to-body weight ratio is then calculated for each animal according to the formula: Liver (g)/BW x 100. Half of the liver is snap-frozen in liquid N_2 for further cytokine analysis (optional), and the remaining 1/2 portion is formalin-fixed for histopathology (optional).

The readouts that are available from PDS for the CDAHFD model in HLCM include body weight, ALT, AST, ALP, T-BIL and ALB levels, liver weight, biomarker analysis (protein or mRNA), and histopathology.

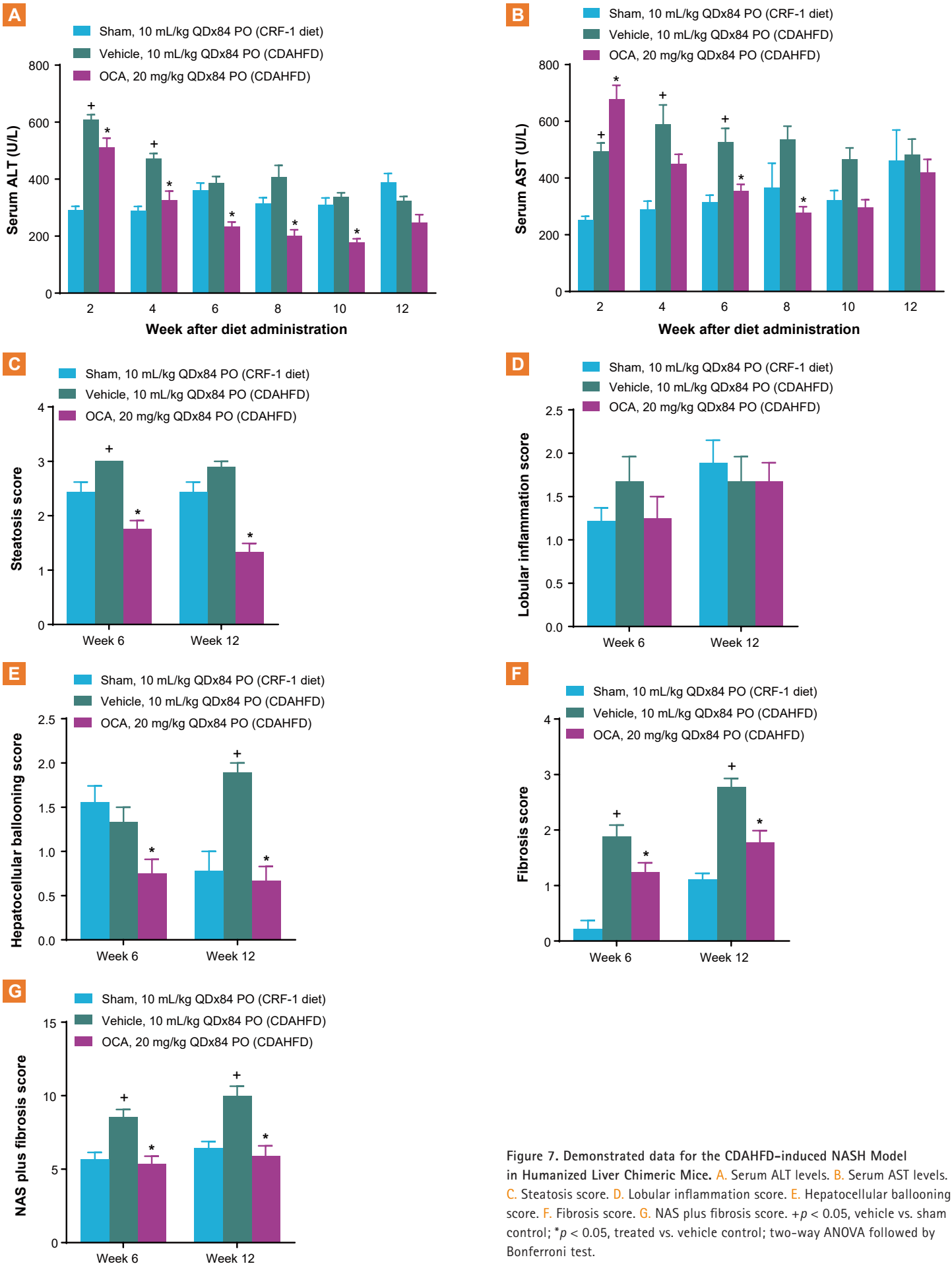

Figure 7. Demonstrated data for the CDAHFD-induced NASH Model in Humanized Liver Chimeric Mice. A. Serum ALT levels. B. Serum AST levels. C. Steatosis score. D. Lobular inflammation score. E. Hepatocellular ballooning score. F. Fibrosis score. G. NAS plus fibrosis score. $+p < 0.05$, vehicle vs. sham control; $*p < 0.05$, treated vs. vehicle control; two-way ANOVA followed by Bonferroni test.

SUMMARY

The complex and not yet fully understood pathogenesis of NASH makes it a challenging disease for effective therapeutic intervention. This is evident by the lack of any FDA-approved therapeutics as of April 2023. Other examples include the recent late-stage clinical failure of elafibranor and the rejection of an NDA for NASH (obeticholic acid) from Intercept Pharmaceuticals in June 2020 (note Intercept filed a new NDA on December 2022 and expects an FDA decision in June 2023). With dozens of candidates in the clinic that target different stages of pathology (e.g., fatty liver, hepatitis, liver fibrosis), efforts to further elucidate disease progression are necessary for success in the clinic. It is also necessary to develop novel *in vitro* assays *and in vivo* models to accurately evaluate NASH drug candidates.

Eurofins Discovery and PDS have both *in vitro* and *in vivo* services to aid clients with their NASH drug discovery programs. The Liver Steatosis, Hepatitis, and Liver Fibrosis LeadHunter Panels provide the opportunity to quickly test compounds across multiple targets, and every assay in each panel can be ordered individually. With several targets, there are multiple assays (e.g., binding, enzymatic, functional, and phenotypic) that may be used to fully interrogate the *in vitro* pharmacological profile of a compound.

Three diet-induced models (MCD and CDAHFD) are validated and available for testing, two in C57BL/6 mice and one in humanized liver chimeric mice (HLCM). Each model reliably induces NAFL, hepatic steatosis, and fibrosis. Induction of fibrosis requires more time in the CDAHFD model, which increases study costs. One benefit of the CDAHFD model is that weight loss does not occur. Due to the fact that mice in the MCD model lose significant body weight, possibly due to suppression of liver stearoyl-coenzyme A desaturase-1 (SCD-1), it may not be used for a long-term study of hepatocellular carcinoma (HCC).[24] The CDAHFD model can be used to study the liver-specific molecular mechanisms responsible for the NAFLD–NASH–HCC progression in a period of 36 weeks.[19] In addition, the CDAHFD model could also be used to investigate the second, or multiple hits, leading to progression of hepatic fibrosis due to excess fat accumulation in the liver. The CDAHFD model in HLCM represents a more clinically relevant model for testing the efficacy of NASH drug candidates. But none of the three models develops obesity or has a metabolic profile in line with human NASH. If drug candidates target obesity or insulin resistance, more suitable *in vivo* models available from PDS include:

Disease Model	Species	Model Number
Obesity, Diet-Induced	Mouse	518510
Type II Diabetes	db/db Mouse	541630
	KK-A^{y} Mouse	541620
	Obese Zucker Diabetic Fatty (ZDF) Rat	541700

Technical Directors and Study Directors are available to consult with clients for their *in vitro* and *in vivo* pharmacology studies. Custom assays or *in vivo* models may also be developed so clients can achieve the specific objectives of their NASH drug discovery program.

For more information on *in vitro* services, please visit: eurofinsdiscovery.com/solution/therapeutic-areas

For more information on *in vivo* models, please visit: pharmacologydiscoveryservices.com

REFERENCES

1. GBD 2017 Cirrhosis Collaborators. The global, regional, and national burden of cirrhosis by cause in 195 countries and territories, 1990-2017: a systematic analysis for the Global Burden of Disease Study 2017. *Lancet Gastroenterol Hepatol.* 2020 Mar;5(3):245-266. doi: 10.1016/S2468-1253(19)30349-8. PMID: 31981519.
2. Estes C, *et al.* Modeling the epidemic of nonalcoholic fatty liver disease demonstrates an exponential increase in burden of disease. *Hepatology.* 2018 Jan;67(1):123-133. doi: 10.1002/hep.29466. PMID: 28802062.
3. Friedman SL, *et al.* Mechanisms of NAFLD development and therapeutic strategies. *Nat Med.* 2018 Jul;24(7):908-922. doi: 10.1038/s41591-018-0104-9. PMID: 29967350.
4. Day CP, James OF. Steatohepatitis: a tale of two "hits"? *Gastroenterology.* 1998 Apr;114(4):842-5. doi: 10.1016/s0016-5085(98)70599-2. PMID: 9547102.
5. Tilg H, Moschen AR. Evolution of inflammation in nonalcoholic fatty liver disease: the multiple parallel hits hypothesis. *Hepatology.* 2010 Nov;52(5):1836-46. doi: 10.1002/hep.24001. PMID: 21038418.
6. Esler WP, Bence KK. Metabolic Targets in Nonalcoholic Fatty Liver Disease. *Cell Mol Gastroenterol Hepatol.* 2019;8(2):247-267. doi: 10.1016/j.jcmgh.2019.04.007. PMID: 31004828.
7. Thiagarajan P, Aithal GP. Drug Development for Nonalcoholic Fatty Liver Disease: Landscape and Challenges. *J Clin Exp Hepatol.* 2019 Jul-Aug;9(4):515-521. doi: 10.1016/j.jceh.2019.03.002. PMID: 31516268.
8. Romero FA, *et al.* The Race to Bash NASH: Emerging Targets and Drug Development in a Complex Liver Disease. *J Med Chem.* 2020 May 28;63(10):5031-5073. doi: 10.1021/acs.jmedchem.9b01701. PMID: 31930920.
9. Roeb E, Geier A. Nonalcoholic steatohepatitis (NASH) - current treatment recommendations and future developments. *Z Gastroenterol.* 2019 Apr;57(4):508-517. English. doi: 10.1055/a-0784-8827. PMID: 30965381.
10. Sumida Y, Yoneda M. Current and future pharmacological therapies for NAFLD/NASH. *J Gastroenterol.* 2018 Mar;53(3):362-376. doi: 10.1007/s00535-017-1415-1. PMID: 29247356.
11. Jahn D, *et al.* Animal models of NAFLD from a hepatologist's point of view. *Biochim Biophys Acta Mol Basis Dis.* 2019 May 1;1865(5):943-953. doi: 10.1016/j.bbadis.2018.06.023. PMID: 29990551.
12. Anstee QM, Goldin RD. Mouse models in non-alcoholic fatty liver disease and steatohepatitis research. *Int J Exp Pathol.* 2006 Feb;87(1):1-16. doi: 10.1111/j.0959-9673.2006.00465.x. PMID: 16436109.
13. Sha W, *et al.* Metabolomic profiling can predict which humans will develop liver dysfunction when deprived of dietary choline. *FASEB J.* 2010 Aug;24(8):2962-75. doi: 10.1096/fj.09-154054. PMID: 20371621.
14. Rinella ME, Green RM. The methionine-choline deficient dietary model of steatohepatitis does not exhibit insulin resistance. *J Hepatol.* 2004 Jan;40(1):47-51. doi: 10.1016/j.jhep.2003.09.020. PMID: 14672613.
15. Kruger AJ, *et al.* Prolonged cenicriviroc therapy reduces hepatic fibrosis despite steatohepatitis in a diet-induced mouse model of nonalcoholic steatohepatitis. *Hepatol Commun.* 2018 Mar 7;2(5):529-545. doi: 10.1002/hep4.1160. PMID: 29761169.
16. Ulmasov B, *et al.* An Inhibitor of Arginine-Glycine-Aspartate-Binding Integrins Reverses Fibrosis in a Mouse Model of Nonalcoholic Steatohepatitis. *Hepatol Commun.* 2018 Dec 27;3(2):246-261. doi: 10.1002/hep4.1298. PMID: 30766962.
17. Lau JK, *et al.* Animal models of non-alcoholic fatty liver disease: current perspectives and recent advances. *J Pathol.* 2017 Jan;241(1):36-44. doi: 10.1002/path.4829. PMID: 27757953.
18. Matsumoto M, *et al.* An improved mouse model that rapidly develops fibrosis in non-alcoholic steatohepatitis. *Int J Exp Pathol.* 2013 Apr;94(2):93-103. doi: 10.1111/iep.12008. PMID: 23305254.
19. Ikawa-Yoshida A, *et al.* Hepatocellular carcinoma in a mouse model fed a choline-deficient, L-amino acid-defined, high-fat diet. *Int J Exp Pathol.* 2017 Aug;98(4):221-233. doi: 10.1111/iep.12240. PMID: 28895242.
20. Erstad DJ, *et al.* Molecular magnetic resonance imaging accurately measures the antifibrotic effect of EDP-305, a novel farnesoid X receptor agonist. *Hepatol Commun.* 2018 May 21;2(7):821-835. doi: 10.1002/hep4.1193. PMID: 30027140.
21. 21. Tateno C. *et al.* Generation of Novel Chimeric Mice with Humanized Livers by Using Hemizygous cDNA-uPA/SCID Mice. *PLoS One.* 2015 Nov 4;10(11):e0142145. doi: 10.1371/journal.pone.0142145. PMID: 26536627.
22. 22. Sugahara G. *et al.* Art of Making Artificial Liver: Depicting Human Liver Biology and Diseases in Mice. *Semin Liver Dis.* 2020 May;40(2):189-212. doi: 10.1055/s-0040-1701444. PMID: 32074631.
23. 23. Kisoh K. *et al.* Estimating Drug Efficacy with a Diet-Induced NASH Model in Chimeric Mice with Humanized Livers. *Biomedicines.* 2021 Nov 9;9(11):1647. doi: 10.3390/biomedicines9111647. PMID: 34829876.
24. Rizki G, *et al.* Mice fed a lipogenic methionine-choline-deficient diet develop hypermetabolism coincident with hepatic suppression of SCD-1. *J Lipid Res.* 2006 Oct;47(10):2280-90. doi: 10.1194/jlr.M600198-JLR200. PMID: 16829692.